This work is under IET copyright and its IET published version may be found in http://www.theiet.org. This file constitutes the draft version.
Work retroactively supported by project TEC2013-47020-C2-2-R (Ministerio de Economia y Competitividad - SPAIN), published in 2014 before the project's official awarding date

Single and Multi-Frequency Wideband Spectrum Sensing with Side-Information

Josep Font-Segura, Gregori Vázquez, and Jaume Riba
Signal Theory and Communications Department
Technical University of Catalonia (UPC)
Jordi Girona 1-3, D5-{214,204,116}Barcelona, Spain
E-mail: {josep-font-segura, gregori.vazquez, jaume.riba}@upc.edu

Abstract

The paper addresses the optimal spectrum sensing detection based on the complete or partial side-information on the signal and noise statistics. The use of the generalized likelihood ratio test (GLRT) involves maximum likelihood (ML) estimation of the nuisances. ML estimation of the unknowns is especially challenging for wideband cognitive radio because closed-form solutions are often not available. Based on the equivalence between the wideband regime and the low-SNR regime, the paper provides a general kernel framework for GLRT spectrum sensing. It is shown that any GLRT detector exclusively depends on the projection of the sample covariance matrix of the data onto a given underlying kernel that reflects the available side-information in the problem. The kernels in several scenarios of interest are derived, including the widespread single and multi-frequency channelization cases. Theoretical interpretations and numerical results show the trade-off between detection performance and the degree of side-information on the most informative statistics for detection, i.e., the modulation format and spectrum distribution of the primary users.

1 Introduction

Today's wireless networks are regulated by a fixed spectrum resource assignment. However, a large portion of this assigned spectrum is used only sporadically by the primary services, while a significant amount of the spectrum remains underutilized [1]. Cognitive radio is a new wireless communication paradigm that utilizes advanced signal processing along with novel dynamic spectrum

policies to support new users who wish to opportunistically communicate in the existing congested spectrum without degrading the established users [2]. For that purpose, a cognitive radio is an adaptive wireless communication system that takes advantage of side-information on the network, e.g., the primary systems activity or channel conditions. Interweave cognitive radio [3] is motivated by opportunistic transmission of secondary users over the available spectrum gaps or holes in given time and geographical location conditions.

The primary function of interweave cognitive radios is to reliably identify the available spectrum resources temporally unused by primary users. This awareness can be obtained through a database, using beacons, or by local spectrum sensing [4]. This paper focuses on spectrum sensing performed at the cognitive radio receivers as it constitutes a broader solution and has less infrastructure requirements. The energy detector, cyclostationarity feature detection, and match-filtering are the most commonly employed techniques for spectrum sensing. However, the performance of such detectors is severely degraded when the side-information on the signal and noise features is incomplete, e.g., the cyclic frequencies. Spectrum sensing detectors based on the generalized likelihood ratio test (GLRT) have received recent attention as the GLRT statistic is optimal in the Neyman-Pearson sense [8] and natively incorporates joint parameter maximum likelihood (ML) estimation for inaccurate model parameters [9]. The effect of side-information on the signal and noise statistics has been reported in [10] in realistic scenarios.

Wideband spectrum sensing has gained recent attention [11]. It is recognized that ML estimation in wideband cognitive radios is especially challenging because wideband regimes are characterized by close to zero spectral efficiency and low signal-to-noise ratios (SNRs) [12]. Furthermore, the method of ML, despite its theoretical appeal, is often difficult to implement, and analytical solutions are not available in many circumstances [13]. However, we show the tractability of the ML formulation in asymptotically low-SNR regimes, and identify that the second-order statistics of the observations are sufficient statistics for the spectrum detection problem when the noise variance is high. In this paper, we derive the optimal ML estimates for GLRT spectrum sensing detection in the single-frequency scenario, and show through low-SNR approximations that any GLRT spectrum sensing detector exclusively depends on a kernel operator and the sample covariance matrix of the observations, asymptotically as the SNR tends to zero. We further extend to cognitive radio networks operating over primary systems that employ multi-frequency communications, such as the terrestrial digital video broadcasting (DVB-T). Simulation results assess the performance comparison of the derived algorithms.

1.1 Main Contribution

The motivation of this work is to reveal an unified structure of GLRT spectrum sensing detectors for wideband cognitive radios, and discuss the application of the proposed framework to several cases of practical interest. We identify that all the optimal wideband spectrum sensing detectors follow, for asymptotically large data records, an underlying framework given by

$$T(X,\Theta) \doteq \int_B \mathcal{K}(\omega,\Theta) P(\omega) d\omega \geq \lambda \tag{1}$$

where Θ represents the set of side-information parameters, $P(\omega)$ is the periodogram of the local observations and B is the sensed bandwidth. Eq. (1) illustrates that any wideband spectrum sensing detector is characterized by an associated kernel $\mathcal{K}(\omega,\Theta)$, which uncovers the fundamental factors that determine the sensing performance. Important remarks on the frequency-domain asymptotic framework (1) are listed below.

- It proves that in asymptotically low-SNR regimes, detection is exclusively based on the second-order treatment of the observations, i.e., on the periodogram $P(\omega)$.
- The kernel has the role of shaping the spectral information contained in the periodogram. As the SNR asymptotically increases, the kernel approaches to a constant and the GLRT behaves as the energy detector. Contrarily, as the SNR asymptotically decreases, the kernel is proportional to the signal power spectral density (PSD) and the GLRT performs a second-order statistics matching between the observations and the model.
- When the signal model parameters are uncertain, the expression of the asymptotic kernel in (1) depends on the ML estimates of the unknowns. As $\mathcal{K}(\omega,\Theta)$ identifies which is the relevant side-information for detection, the degradation incurred by the estimation is related to the performance of the detection.

1.2 Related Work

A numerous amount of spectrum sensing detectors based on the GLRT have been reported in the last years. It is a well-known signal processing result that in the low-SNR regime, the second-order statistics of the signal and noise involved in the detection are sufficient statistics for detection [14]. More precisely, the cross-correlation between signal and noise can be exploited in the frequency, spatial, or temporal domains.

Firstly, frequency correlation detectors are intended to uncover the spectral coherence of cyclostationary processes (see [15] and the references thereby). However, these detectors are very sensitive to the signal and noise features, and require in general high computational complexity. A spectral feature based detector has been reported in [16].

Secondly, a bunch of signal detectors that exploit spatial correlation have been proposed in the recent literature [17–28]. Addressing the GLRT problem in the multiple antenna framework has allowed the formulation of well-known Gaussian detectors such as the arithmetic-to-geometric (AGM) detector [17], rank-1 detectors [20, 24, 27], the rank-P detector [22], and the locally most powerful invariant test (LMPIT) [26]. In the case of fading, the algorithms reported in [18, 19, 23] address blind detection with unknown channel parameters, whereas the works by [21, 25, 28] investigate the use of prior information in the detection process. The common frawmework of [17–28] is that the detectors are based on the eigenvalue decomposition of the spatial correlation matrix. Therefore, these algorithms are only valid when the secondary users are equipped with multiple antennas.

Thirdly, the exploitation of temporal correlation has gained little attention, even though temporal correlation matrices exhibit good properties of stability and computational complexity. Related work involving GLRT detection include [29–31]. In [29], the sensitivity of oversampled temporal correlation based detection to frequency offsets is investigated. In order to further improve efficiency, [30] reports a detector based on the Cholesky factorization of the sample correlation matrix, whereas the work by [31] is concerned in performing signal detection while communicating at the same time. These works does not consider side-information on the primary signal correlation.

In this work, the temporal correlation of the primary users is exploited given the Toeplitz structure of the correlation matrices when one single antenna is employed at the cognitive receiver. An $N \times N$ Hermitian Toeplitz matrix has only N degrees of freedom. Therefore, the algorithms derived in this paper will have good properties of stability and computational complexity. We note that the detection of a stationary process with a single antenna constitutes a well-defined fundamental problem by itself, which takes advantage of the second-order statistics distinctness between hypotheses. Partial results of this paper have been originally presented in [33, 34].

1.3 Paper Outline

The rest of the paper is organized as follows. Section 2 describes the spectrum sensing cognitive radio problem and its asymptotic frequency-domain interpretation. The single-frequency GLRT

detectors with known and with unknown noise variance are derived in Section 3 and 4, respectively. An extension to multi-frequency systems is discussed in Section 5. Section 6 provides performance comparisons by means of numerical simulations, and Section 7 concludes the paper.

2 Signal Model and Problem Statement

We consider the spectrum sensing problem of a wideband cognitive radio network monitoring the activity of the primary users' signal, denoted by $S(t)$, over the sensed spectrum of bandwidth B. The sensed signal at the local cognitive radio is $X(t) = S(t) + W(t)$, where $W(t)$ is the double-sided complex zero-mean additive white Gaussian noise with spectral density $N_0/2$. In this paper, a block processing of the signal is considered. On the one hand, the N-dimensional discrete-time received signal is defined as $\mathbf{x}[m] \doteq [X(t_1^m), \ldots, X(t_N^m)]^T$, where the sampling instants satisfy Nyquist uniform sampling. On the other hand, each cognitive radio acquires M blocks given by $\mathbf{X} \doteq (\mathbf{x}[1], \ldots, \mathbf{x}[M])$. Therefore, the block size N is a side-information parameter large enough to cope with the temporal correlation of the primary signal, and M is a factor to improve the performance of the detectors by averaging independent blocks. Matrices $\mathbf{S}$ and $\mathbf{W}$ are similarly defined.

The spectrum sensing problem may be therefore cast as the binary hypothesis testing problem

$$\begin{aligned} \mathcal{H}_0 &: \mathbf{X} = \mathbf{W} \\ \mathcal{H}_1 &: \mathbf{X} = \mathbf{S} + \mathbf{W}, \end{aligned} \tag{2}$$

where $\mathcal{H}_0$ is the signal-free hypothesis, and $\mathcal{H}_1$ is the signal-present hypothesis. In (2), the column-entries of the signal and noise observations are complex multivariate zero-mean Gaussian distributed with correlation matrices $\mathbf{R}_s = \gamma \mathbf{R}_0$, and $\mathbf{R}_w = \sigma^2 \mathbf{I}$, respectively, with $\mathbf{R}_0$ the normalized signal correlation matrix such that $\mathrm{tr}(\mathbf{R}_0) = N$. We further define the detection SNR as $\rho_0 \doteq \frac{\gamma}{\sigma^2}$. In the problem at hand, it is a valid assumption that both noise and signal are normally distributed. While facilitating the analysis, this is reasonable because $S(t)$ is the superposition of no-LOS signals (holding the the central limit theorem), but also because Gaussian ML estimation provides, asymptotically as $\rho_0 \to 0$, the optimum second-order estimator [35]. As the size of the spectrum portion taken into consideration increases, the relative overall occupation of primary systems becomes low, which motivates the derivation of robust spectrum sensing detectors focused on low-SNR regimes. Therefore, throughout the paper we will assume that asymptotically $\rho_0 \to 0$, where ρ_0 is the nominal SNR at detection.

We are interested in detecting the presence of the signal $\mathbf{S}$ based on the local observations $\mathbf{X}$ in (2). It is known that the GLRT is asymptotically optimal in the Neyman-Pearson sense, i.e., to maximize the probability of detection for a given probability of false alarm level [8]. Let Ψ_0 and Ψ_1 denote the unknown model parameters under $\mathcal{H}_0$ and $\mathcal{H}_1$, respectively. The optimal test in the Neyman-Pearson sense for deciding between hypotheses $\mathcal{H}_0$ and $\mathcal{H}_1$ is given by

$$L(\mathbf{X}, \Theta) \doteq \frac{p(\mathbf{X}|\hat{\Psi}_1, \Theta_1, \mathcal{H}_1)}{p(\mathbf{X}|\hat{\Psi}_0, \Theta_0, \mathcal{H}_0)} \geq \lambda, \tag{3}$$

where the ML estimates of the unknown parameters are given by $\hat{\Psi}_0 = \arg\max_{\Psi} p(\mathbf{X}|\Psi, \Theta_0, \mathcal{H}_0)$, and $\hat{\Psi}_1 = \arg\max_{\Psi} p(\mathbf{X}|\Psi, \Theta_1, \mathcal{H}_1)$, respectively. In (3), Θ denotes the set of side-information parameters, and $\Theta_1, \Theta_0 \subseteq \Theta$. The threshold λ sets the decision level for which the test $L(\mathbf{X}, \Theta) \geq \lambda$ decides for $\mathcal{H}_1$, and for $\mathcal{H}_0$ otherwise, and is selected to satisfy the false alarm level $\mathbb{P}(\mathcal{H}_1|\mathcal{H}_0) = \mathbb{P}(L(\mathbf{X}, \Theta) \geq \lambda|\mathcal{H}_0) = \alpha$. Despite its theoretical appeal, the ML estimation and GLRT detection in (3) are often difficult to implement, and analytical solutions are not available in many circumstances [13]. However, we show that GLRT spectrum sensing detection for wideband cognitive radio is encompassed in a low-complex unified framework. In particular, it is shown that for asymptotically $\rho_0 \to 0$, the GLRT (3) is of the form

$$T(\mathbf{X}, \Theta) \doteq \frac{1}{M} \log L(\mathbf{X}, \Theta) \approx \mathrm{tr}\left(\mathbf{K}(\Theta)\hat{\mathbf{R}}_x\right) \geq \lambda, \tag{4}$$

where $\hat{\mathbf{R}}_x$ is the sample covariance matrix of $\mathbf{X}$, $\mathbf{K}$ constitutes the kernel associated to the detector, and λ is the detection threshold. By further resorting to large data records, i.e., for $N \to \infty$, the statistic (4) is asymptotically equivalent to the following expression in the frequency-domain

$$T(\mathbf{X}, \Theta) \doteq \int_B \mathcal{K}(\omega, \Theta) P(\omega) d\omega \geq \lambda, \tag{5}$$

where $\mathcal{K}(\omega, \Theta)$ is a kernel associated to each detector, $P(\omega)$ is the continuous-frequency periodogram of $\mathbf{X}$. Furthermore, any GLRT spectrum sensing detector only depends, asymptotically as $\rho_0 \to 0$, on the second-order statistics of the observations. A sketch of the proof of (4) and (5) is reported in Appendix A.

From (5), we deduce that wideband spectrum sensing is strictly based on the second-order statistics of the observations shaped by a kernel that highlights the signal and noise features which are relevant for detection. Moreover, we show that frequency-domain asymptotic kernels have a common inner structure that depends on the signal and interference plus noise statistics. Let $\phi_s(\omega)$ and $\phi_\nu(\omega)$ denote the PSD of the signal to be detected and the interference plus noise, respectively.

The detection kernel in (5) has an internal structure given by (see Appendix A):

$$\mathcal{K}_0\left[\phi_s(\omega), \phi_\nu(\omega)\right] \doteq \frac{1}{\phi_\nu(\omega)} \frac{\phi_s(\omega)}{\phi_s(\omega) + \phi_\nu(\omega)}, \tag{6}$$

which will be used in subsequent sections to provide a unified perspective of different approaches to the spectrum sensing problem. In the high-SNR regime, the kernel approaches to $\frac{1}{\phi_\nu(\omega)}$ and the detector asymptotically behaves as the energy detector with noise PSD given by $\phi_\nu(\omega)$. On the other hand, we show that the kernel becomes proportional to $\frac{\phi_s(\omega)}{\phi_\nu^2(\omega)}$ as the interference plus noise increases, and the detector performs the spectral correlation between the periodogram of the observations and the signal PSD weighted by the inverse of the squared spectrum of the interference plus noise. This result corresponds to the locally optimum detector for the cognitive radio problem (2), obtained through expanding the optimum quadratic statistic in the low-SNR limit [5].

3 Single-Frequency Wideband Spectrum Sensing with Known Noise Variance

In this section, we derive the optimal single-frequency GLRT detectors based on the assumption that noise variance present at the cognitive radio receiver is known. This is a valid assumption in most cognitive radio networks, as the control layers set predetermined silent periods devoted to threshold computation.

3.1 Estimator-Correlator

The optimal test with known parameters is the estimator-correlator, given by [14, Eq. (5.16)]

$$T_1(\mathbf{X}|\mathbf{R}_s, \sigma^2) = \frac{1}{\sigma^2}\mathrm{tr}\left(\mathbf{R}_s(\mathbf{R}_s + \sigma^2\mathbf{I})^{-1}\hat{\mathbf{R}}_x\right) \geq \lambda_1, \tag{7}$$

where $\hat{\mathbf{R}}_x$ stands for the sample covariance matrix, i.e., $\hat{\mathbf{R}}_x \doteq \frac{1}{M}\sum_m \mathbf{x}_m\mathbf{x}_m^H$. The detector (7) is a classical detection result, which correlates the observations with the output of the Wiener filter or minimum mean square error (MMSE) estimate of the signal, i.e., with the term $\mathbf{R}_s(\mathbf{R}_s + \sigma^2\mathbf{I})^{-1}\mathbf{x}_m$. The frequency-domain asymptotic interpretation of the estimator-correlator has recently been studied in [32], from which we identify that the kernel associated to the estimator-correlator is given by $\mathcal{K}_1(\omega, \phi_s, \sigma^2) = \mathcal{K}_0\left[\phi_s(\omega), \sigma^2\right]$. We note that (7) and its associated kernel symbolize an upper-bound on the sensing performance of GLRT spectrum sensing detectors, and therefore provide a fundamental limit useful for performance assessments.

3.2 Signal Level Detector

This assumption represents a more realistic scenario, as the power at which the primary users' signal reaches the cognitive radio receiver is an unknown parameter. Under the white noise assumption, the presence of correlation in the observations can be further exploited by the spectrum sensing algorithm to detect the presence of this signal. For a given normalized signal correlation matrix $\mathbf{R}_0$, the optimal GLRT spectrum sensing detector in the wideband regime with known noise variance is given by

$$T_2(\mathbf{X}|\mathbf{R}_0,\sigma^2) = \frac{1}{\sigma^2}\mathrm{tr}\left(\hat{\gamma}\mathbf{R}_0(\hat{\gamma}\mathbf{R}_0+\sigma^2\mathbf{I})^{-1}\hat{\mathbf{R}}_x\right) \geq \lambda_2, \tag{8}$$

where the ML estimate of the signal level, derived in Appendix B.1, is given by

$$\hat{\gamma} = \left(\frac{\mathrm{tr}(\mathbf{R}_0\hat{\mathbf{R}}_x)-\sigma^2 N}{\mathrm{tr}(\mathbf{R}_0^2)}\right)^+, \tag{9}$$

where the operator $(\cdot)^+$ is defined as $(x)^+ \doteq \max(0,x)$.

The evaluation and comparison of (8) in front of (7) uncovers that the kernel $\mathcal{K}_2(\omega,\phi_0,\sigma^2) = \mathcal{K}_0\left[\hat{\gamma}\phi_0(\omega),\sigma^2\right]$ is based on the ML estimate of the signal level γ. From the frequency-domain asymptotic interpretation of (9), we deduce that kernel exploits the correlated structure of $\mathbf{R}_0$ and the side-information on the noise variance to recover γ. We emphasize that the correlated structure of $\mathbf{R}_0$ is only required for unknown noise variance (c.f. Section 4.B), whereas the estimate (9) is still valid even for white signal, i.e., $\mathbf{R}_0$ a diagonal matrix, when the noise variance is known.

3.3 Toeplitz Detector

We next discuss the spectrum sensing detection problem when the primary users' signal correlation matrix is unknown. According to the GLRT formulation, under $\mathcal{H}_1$ an estimate of $\mathbf{R}_s$ based on the local observations is required to perform the detection. Because $\mathbf{R}_s$ represents the correlation of a stationary signal, it is the solution to ML estimate problem with the additional constraints $\mathbf{R}_s \succeq \mathbf{0}$ and complex Hermitian Toeplitz structure. Any complex Hermitian Toeplitz matrix of order N is represented by a unique vector of length N containing, e.g., the element of the first row of the matrix. A direct consequence of this property is that $\mathbf{R}_s$ has only N degrees of freedom and, then, it can uniquely be represented by the N first correlation lags, $(r_s[0],\ldots,r_s[N-1])$. However, for the problem at hand, we propose the following decomposition for complex Hermitian Toeplitz matrices

$$\mathbf{R}[\boldsymbol{\beta}] = \beta_0\mathbf{T}_0 + \sum_{n=1}^{N-1}\left(\beta_n\mathbf{T}_n^T + \beta_n^*\mathbf{T}_n\right), \tag{10}$$

where $\boldsymbol{\beta} \doteq (\beta_0, \ldots, \beta_{N-1})$ are the N coefficients that uniquely represent the matrix $\mathbf{R}$ onto the orthogonal basis $\mathcal{T} \doteq \{\mathbf{T}_n\}$ of the space of complex Hermitian Toeplitz matrices. We note that $\mathrm{tr}(\mathbf{T}_i \mathbf{T}_j^T) \propto \delta_{ij}$, where δ_{ij} is the Kronecker delta, i.e., $\delta_{ij} = 1$ if $i = j$ and 0 otherwise.

For a given Toeplitz orthogonal basis $\mathcal{T} = \{\mathbf{T}_n\}$, the optimal GLRT spectrum sensing detector in the wideband regime with known noise variance is given by

$$T_3(\mathbf{X}|\mathcal{T}, \sigma^2) = \frac{1}{\sigma^2} \mathrm{tr}\left(\mathbf{R}_s[\hat{\boldsymbol{\beta}}](\mathbf{R}_s[\hat{\boldsymbol{\beta}}] + \sigma^2 \mathbf{I})^{-1} \hat{\mathbf{R}}_x\right) \geq \lambda_3, \tag{11}$$

where the coefficients of $\hat{\mathbf{R}}_s$ onto $\mathcal{T}$, derived in Appendix B.2, are given by

$$\hat{\beta}_0 = \left(\frac{1}{N}\mathrm{tr}(\hat{\mathbf{R}}_x) - \sigma^2\right)^+ \tag{12a}$$

$$\hat{\beta}_n = \frac{\mathrm{tr}(\mathbf{T}_n \hat{\mathbf{R}}_x)}{\mathrm{tr}(\mathbf{T}_n \mathbf{T}_n^T)}, \quad 1 \leq n \leq N-1. \tag{12b}$$

It is noticed that when employing diagonal matrices, i.e., $\mathbf{T}_0 = \mathbf{I}$, and $\mathbf{T}_n$ all-zeros matrix with an all-ones semi-diagonal n-positions above the main diagonal, the coefficients β_n have the physical meaning of the correlation lags, i.e., $\hat{\beta}_n = \hat{r}_s[n]$, for $0 \leq n \leq N-1$. Therefore, the computation of the zero-lag β_0 in (12a) is based on the detected energy and the side-information on the noise variance. Conversely, because $\mathrm{tr}(\mathbf{T}_n) = 0$ for $n > 0$, each coefficient β_n in (12b) uncovers the stationary part of the received observations, i.e., takes into account the off-diagonal information contained in $\hat{\mathbf{R}}_x$. The kernel associated to (11) is given by $\mathcal{K}_3(\omega, \mathcal{T}, \sigma^2) = \mathcal{K}_0\left[\left(\hat{\beta}_0 + \sum_{n=1}^{N-1} \mathrm{Re}(\hat{\beta}_n)\psi_n(\omega)\right)^+, \sigma^2\right]$, where $\psi_n(\omega)$ is spectral density associated to the correlation matrices $(\mathbf{T}_n + \mathbf{T}_n^T)$, and $\mathrm{Re}(z)$ takes the real part of $z \in \mathbb{C}$. The GLRT spectrum sensing detector (11) exploits the side-information on the noise variance to perform optimal matching between the observations and the frequency patterns ψ_n. When noting that $\sigma^2 + \hat{\beta}_0$ is the energy detector, it is appreciated that the detection takes advantage of the frequency variations of the periodogram. Hence, it is expected to achieve performance gain with respect to the energy detector.

4 Single-Frequency Wideband Spectrum Sensing with Unknown Noise Variance

Many detectors, including the energy detector, assume exact side-information on the noise variance to properly perform the detection. Yet in practice, a mismatch on the noise variance may significantly degrade the sensing performance of the detectors, as reported in [36]. For this purpose, we

extend the single-frequency GLRT spectrum sensing detectors derived in Section 3 for unknown noise variance. Under $\mathcal{H}_0$, the ML estimate of σ^2 is given by [14, Eq. (9.10)] as $\hat{\sigma}_0^2 = \frac{1}{N}\text{tr}(\hat{\mathbf{R}}_x)$.

4.1 Noise Variance Detector

We first assume perfect side-information on the signal correlation matrix $\mathbf{R}_s$. The ML estimate of σ^2 under $\mathcal{H}_1$ is derived in [14, Section 9.4] for the low-SNR regime, and is given by

$$\hat{\sigma}_1^2 = \frac{1}{N}\left[\text{tr}\left(\hat{\mathbf{R}}_x - \mathbf{R}_s\right)\right]^+. \tag{13}$$

For a given signal correlation matrix $\mathbf{R}_s$, the optimal GLRT spectrum sensing detector in the wideband regime with unknown noise variance is given by

$$T_4(\mathbf{X}|\mathbf{R}_s) = \frac{1}{\hat{\sigma}_1^2}\text{tr}\left(\mathbf{R}_s(\hat{\sigma}_1^2\mathbf{I} + \mathbf{R}_s)^{-1}\hat{\mathbf{R}}_x\right) \geq \lambda_4, \tag{14}$$

where the ML estimate of the noise variance under $\mathcal{H}_1$ is given by (13).

The side-information on $\mathbf{R}_s$ is twofold. On the one hand, recalling that the kernel associated to (14) is $\mathcal{K}_4(\omega, \phi_s) = \mathcal{K}_0\left[\phi_s(\omega), \hat{\sigma}_1^2\right]$, it is noted that the side-information pattern for detecting primary systems is supplied by $\phi_s(\omega)$. On the other hand, the side-information on the energy of $\phi_s(\omega)$ diminishes the problem of noise mismatching, as the estimate of the noise variance is based on both the received observations and $\phi_s(\omega)$.

4.2 Signal Level and Noise Variance Detector

We next consider spectrum sensing problem when the cognitive radio receivers have perfect side-information on the normalized signal correlation matrix, $\mathbf{R}_0$. Hence, based on the structure of $\mathbf{R}_0$, the optimal GLRT spectrum sensing detector aims at recover both the signal level and noise variance. For a given normalized signal correlation matrix $\mathbf{R}_0$, the optimal GLRT spectrum sensing detector in the wideband regime with unknown noise variance is given by

$$T_5(\mathbf{X}|\mathbf{R}_0) = \frac{1}{\hat{\sigma}_1^2}\text{tr}\left(\hat{\gamma}\mathbf{R}_0(\hat{\sigma}_1^2\mathbf{I} + \hat{\gamma}\mathbf{R}_0)^{-1}\hat{\mathbf{R}}_x\right) \geq \lambda_5, \tag{15}$$

where the ML estimates of the signal level and noise variance, derived in Appendix B.3, read

$$\hat{\gamma} = \left(\frac{\text{tr}\left(\hat{\mathbf{R}}_x(\mathbf{R}_0 - \mathbf{I})\right)}{\text{tr}(\mathbf{R}_0^2) - N}\right)^+ \tag{16a}$$

$$\hat{\sigma}_1^2 = \left(\frac{1}{N}\text{tr}(\hat{\mathbf{R}}_x) - \hat{\gamma}\right)^+. \tag{16b}$$

The ML estimates of γ and σ^2 under $\mathcal{H}_1$ provide further insight on the sensing performance of the test statistic (15). It is first observed that (16a) is proportional to $\mathrm{tr}(\hat{\mathbf{R}}_x\mathbf{R}_0^{\mathrm{OFF}})$, where $\mathbf{R}_0^{\mathrm{OFF}}$ is the diagonal off-loaded correlation matrix of the primary users' signal, defined as $\mathbf{R}_0^{\mathrm{OFF}} \doteq \mathbf{R}_0 - \mathbf{I}$. Under the stationarity assumption, we outline that (16a) is an energy detector that takes into account solely the statistics of the received observations that are not affected by the noise, i.e., the presence of non-zero correlation lags. Conversely, if the primary users' signal is cyclostationary, the main diagonal of $\mathbf{R}_0$ is not uniform, and (16a) evaluates the variability around the mean of the main diagonal. In conclusion, the ML estimate of the signal level is a linear combination of a measure of the instantaneous energetic variability and a measure of the degree of autocorrelation present in the non-zero lags. Similar interpretations can be obtained in view of the asymptotic associated kernel $\mathcal{K}_5(\omega, \phi_0) = \mathcal{K}_0\left[\hat{\gamma}\phi_0(\omega), \hat{\sigma}_1^2\right]$.

4.3 Toeplitz and Noise Variance Detector

Finally, we discuss the optimal spectrum sensing detector when the signal correlation matrix is fully unknown to the cognitive radio receivers with the additional constraint of complex Hermitian Toeplitz structure. For a given Toeplitz orthogonal basis $\mathcal{T}$, the optimal GLRT spectrum sensing detector in the wideband regime with unknown noise variance is given by

$$T_6(\mathbf{X}|\mathcal{T}) = \frac{1}{\hat{\sigma}_1^2 + \hat{\beta}_0}\mathrm{tr}\left(\mathbf{R}_s[\hat{\boldsymbol{\beta}}_1](\hat{\sigma}_1^2\mathbf{I} + \mathbf{R}_s[\hat{\boldsymbol{\beta}}_1])^{-1}\hat{\mathbf{R}}_x\right) \geq \lambda_6, \tag{17}$$

where $\boldsymbol{\beta}_1 \doteq (0, \beta_1, \ldots, \beta_{N-1})$, and the ML estimates of the noise variance and the coefficients of $\hat{\mathbf{R}}_s$ onto $\mathcal{T}$, derived in Appendix B.4, are given by

$$\hat{\beta}_0 + \hat{\sigma}_1^2 = \frac{1}{N}\mathrm{tr}(\hat{\mathbf{R}}_x) \tag{18a}$$

$$\hat{\beta}_n = \frac{\mathrm{tr}(\mathbf{T}_n\hat{\mathbf{R}}_x)}{\mathrm{tr}(\mathbf{T}_n\mathbf{T}_n)}, \quad 1 \leq n \leq N-1. \tag{18b}$$

The frequency-domain asymptotic interpretation of (17) can be outlined from its associated kernel, which is given by $\mathcal{K}_6(\omega, \mathcal{T}) = \mathcal{K}_0\left[\left(\sum_{n=1}^{N-1}\mathrm{Re}(\hat{\beta}_n)\psi_n(\omega)\right)^+, \hat{\beta}_0 + \hat{\sigma}_1^2\right]$. When releasing the structure of $\mathbf{R}_0$, we observe that the test statistic (17) cannot separate the signal and noise energy contributions, because (18a) is treated as interference plus noise. As a consequence, the sensing performance depends on the variability of the periodogram, i.e., the contributions of the patterns $\psi_n(\omega)$, for $n \geq 1$, with respect to the total received energy.

5 Multi-Frequency Spectrum Sensing

We next consider the spectrum sensing problem for cognitive radio systems where the primary users' services employ frequency-division multiplexing (FDM) with predetermined channelization. The sensed multi-frequency system is characterized by K adjacent channels, and hence the sampled baseband observations admit the multi-frequency structure

$$\mathbf{x}[m] = \sum_{k=1}^{K} \mathbf{s}_k[m] + \mathbf{w}[m], \tag{19}$$

for $1 \leq m \leq M$, where $\mathbf{s}_k$ denotes the received signal located at the k-th channel, and $\mathbf{w}$ is the complex zero-mean additive white Gaussian noise with variance σ^2. The statistics of $\mathbf{s}_k$ are modeled as complex zero-mean Gaussian with correlation matrix $\gamma_k \mathbf{R}_k$, where γ_k stands for the received power level on the k-th channel, and $\mathbf{R}_k$ is the normalized Toeplitz correlation matrix of the primary users' signal on the k-th channel, with $\mathrm{tr}(\mathbf{R}_k) = N$. If the sensed multi-frequency system employs homogeneous services, the signal statistics across channels further accomplish $\mathbf{R}_k = \mathbf{R}_0 \odot (\mathbf{e}(\omega_k)\mathbf{e}^H(\omega_k))$, where $\mathbf{R}_0$ is the baseband basic modulation format, and $\mathbf{e}(\omega)$ is the frequency vector at ω, i.e., $\mathbf{e}^H(\omega) \doteq \begin{bmatrix} 1 & e^{\jmath\omega} & \dots & e^{\jmath\omega(N-1)} \end{bmatrix}$. Let $\mathbf{R}_s[\boldsymbol{\gamma}] \doteq \sum_{k=1}^{K} \gamma_k \mathbf{R}_k$. For notation purposes, we define $\mathcal{M} = \{\mathbf{R}_k\}$ as the set of normalized multi-frequency correlation matrices, and $\boldsymbol{\gamma} \doteq (\gamma_1, \dots, \gamma_K)^T$.

5.1 Nuisance-Hypothesis Testing

The spectrum sensing problem for multi-frequency signals involves a joint multiple-hypotheses test [14], which evaluates the $2^K - 1$ possible combinatorial occupation of occupations. Hence, the complexity of multiple-hypotheses testing grows exponentially with the number of channels and becomes an impractical approach. It is noticed that spectrum sensing on the k-th channel is governed by the signal level γ_k. Therefore, we can treat (19) as a nuisance-hypotheses testing problem. Let $\mathcal{H}_{1,k}$ and $\mathcal{H}_{0,k}$ denote the hypotheses representing the primary system transmitting or not transmitting over the k-th channel, respectively. We define $\boldsymbol{\gamma}_{\bar{k}} \doteq (\gamma_1, \dots, \gamma_{k-1}, 0, \gamma_{k+1}, \dots, \gamma_K)^T$, for $1 \leq k \leq K$. The nuisance-hypotheses testing problem at the k-th channel is then given by

$$L_k(\mathbf{X}, \Theta) = \frac{p(\mathbf{X}|\hat{\boldsymbol{\gamma}}, \Theta_1, \mathcal{H}_{1,k})}{p(\mathbf{X}|\hat{\boldsymbol{\gamma}}_{\bar{k}}, \Theta_0, \mathcal{H}_{0,k})} \geq \lambda_k, \tag{20}$$

for $1 \leq k \leq K$. The complexity has been reduced to a set of K binary tests.

5.2 Multi-Frequency Detector

Assume that each cognitive radio device has perfect side-information on the noise variance σ^2, as well as the primary system multi-frequency structure $\mathcal{M}$. For a given multi-frequency system $\mathcal{M}$, the optimal GLRT spectrum sensing detector at the k-th channel in the wideband regime with known noise variance is given by

$$T_{7,k}(\mathbf{X}|\mathcal{M},\sigma^2) = \mathrm{tr}\left(\hat{\gamma}_k \boldsymbol{\Xi}_k^{-1}\mathbf{R}_k(\hat{\gamma}_k\mathbf{R}_k + \boldsymbol{\Xi}_k)^{-1}\hat{\mathbf{R}}_x\right) \geq \lambda_{7,k}, \tag{21}$$

where $\boldsymbol{\Xi}_k \doteq \sum_{l\neq k}\hat{\gamma}_l\mathbf{R}_l + \sigma^2\mathbf{I}$, and the ML estimates of the signal levels, derived in [33, Appendix B], are given by the solution to [1]

$$\begin{pmatrix} \mathrm{tr}(\mathbf{R}_1^2) & \dots & \mathrm{tr}(\mathbf{R}_1\mathbf{R}_K) \\ \vdots & & \vdots \\ \mathrm{tr}(\mathbf{R}_K\mathbf{R}_1) & \dots & \mathrm{tr}(\mathbf{R}_K^2) \end{pmatrix} \times \begin{pmatrix} \gamma_1 \\ \vdots \\ \gamma_K \end{pmatrix} = \begin{pmatrix} \mathrm{tr}(\mathbf{R}_1\hat{\mathbf{R}}_x) \\ \vdots \\ \mathrm{tr}(\mathbf{R}_K\hat{\mathbf{R}}_x) \end{pmatrix} - \sigma^2 N\mathbf{1}, \tag{22}$$

where $\mathbf{1}$ is the all-ones column vector.

We note that when the number of available samples is small, the orthogonality between channels is not preserved and, in general, the system of equations (22) is coupled because $\mathrm{tr}(\mathbf{R}_k\mathbf{R}_l) \neq 0$, for $l \neq k$. However, for large data records, the system matrix in (22) becomes nearly diagonal, and the ML estimates at each channel are independent on the other channels, giving $\mathrm{tr}(\mathbf{R}_k^2)\hat{\gamma}_k = \mathrm{tr}(\mathbf{R}_k\hat{\mathbf{R}}_x) - \sigma^2 N$. In both cases, the coefficients $\mathrm{tr}(\mathbf{R}_k\mathbf{R}_l)$ in (22) can be computed off-line. The frequency-domain asymptotic kernel for the spectrum sensing detection at the k-th channel is given by $\mathcal{K}_{7,k}(\omega,\mathcal{M},\sigma^2) = \mathcal{K}_0\left[\hat{\gamma}_k\phi_k(\omega), \sum_{l\neq k}\hat{\gamma}_l\phi_l(\omega) + \sigma^2\right]$. We see that the detector employs the relative occupation on the remaining frequencies as interference for sensing the k-th channel. As expected, the performance of (21) is affected by the signal-to-interference-plus-noise ratio (SINR) based on the cross-correlation that arises from the adjacent channels. We finally highlight that (21) and (22) are a generalization of the wideband signal level detector (8) and the estimate (9).

5.3 Multi-Frequency and Noise Variance Detector

We finally consider the detection of multi-frequency systems with unknown noise variance. For a given multi-frequency system $\mathcal{M}$, the optimal GLRT spectrum sensing detector at the k-th channel

[1] Solving for $\boldsymbol{\gamma}$ in (22) requires either solving the system of equations or computing the inverse of the system matrix. In both cases, the cognitive radio user can make use of efficient algorithms given the symmetry properties of the problem.

Table 1: Summary of GLRT Spectrum Sensing Detectors' Kernels and ML Estimates

Detector	Test Statistic	Equation No.	Asymptotic Kernel	ML Estimates
Estimator-Correlator	$T_1(\mathbf{X}\|\mathbf{R}_s,\sigma^2)$	(7)	$\mathcal{K}_0\left[\phi_s(\omega),\sigma^2\right]$	-
Signal Level	$T_2(\mathbf{X}\|\mathbf{R}_0,\sigma^2)$	(8)	$\mathcal{K}_0\left[\hat{\gamma}\phi_0(\omega),\sigma^2\right]$	(9)
Toeplitz	$T_3(\mathbf{X}\|\mathcal{T},\sigma^2)$	(11)	$\mathcal{K}_0\left[\hat{\beta}_0+\sum_{n=1}^{N-1}\mathrm{Re}(\hat{\beta}_n)\psi_n(\omega),\sigma^2\right]$	(12)
Noise Level	$T_4(\mathbf{X}\|\mathbf{R}_s)$	(14)	$\mathcal{K}_0\left[\phi_s(\omega),\hat{\sigma}_1^2\right]$	(13)
Signal and Noise Levels	$T_5(\mathbf{X}\|\mathbf{R}_0)$	(15)	$\mathcal{K}_0\left[\hat{\gamma}\phi_0(\omega),\hat{\sigma}_1^2\right]$	(16)
Toeplitz and Noise Level	$T_6(\mathbf{X}\|\mathcal{T})$	(17)	$\mathcal{K}_0\left[\sum_{n=1}^{N-1}\mathrm{Re}(\hat{\beta}_n)\psi_n(\omega),\hat{\beta}_0+\hat{\sigma}_1^2\right]$	(18)
Multi-Frequency	$T_{7,k}(\mathbf{X}\|\mathcal{M},\sigma^2)$	(21)	$\mathcal{K}_0\left[\hat{\gamma}_k\phi_k(\omega),\sum_{l\neq k}\hat{\gamma}_l\phi_l(\omega)+\sigma^2\right]$	(22)
Multi-Frequency Noise	$T_{8,k}(\mathbf{X}\|\mathcal{M})$	(23)	$\mathcal{K}_0\left[\hat{\gamma}_k\phi_k(\omega),\sum_{l\neq k}\hat{\gamma}_l\phi_l(\omega)+\hat{\sigma}_1^2\right]$	(24)

in the wideband regime with unknown noise variance is given by

$$T_{8,k}(\mathbf{X}|\mathcal{M}) = \mathrm{tr}\left(\mathbf{\Xi}_k^{-1}\hat{\gamma}_k\mathbf{R}_k(\hat{\gamma}_k\mathbf{R}_k+\mathbf{\Xi}_k)^{-1}\hat{\mathbf{R}}_x\right) \geq \lambda_{8,k}, \tag{23}$$

where $\mathbf{\Xi}_k \doteq \sum_{l\neq k}\hat{\gamma}_l\mathbf{R}_l+\hat{\sigma}_1^2\mathbf{I}$, and the ML estimates of the signal levels and noise variance, derived in [33, Appendix C], are given by

$$\begin{pmatrix} \mathrm{tr}(\mathbf{R}_1^2) & \dots & \mathrm{tr}(\mathbf{R}_1\mathbf{R}_K) & N \\ \vdots & & \vdots & \vdots \\ \mathrm{tr}(\mathbf{R}_K\mathbf{R}_1) & \dots & \mathrm{tr}(\mathbf{R}_K^2) & N \\ N & \vdots & N & N \end{pmatrix} \times \begin{pmatrix} \gamma_1 \\ \vdots \\ \gamma_K \\ \sigma_1^2 \end{pmatrix} = \begin{pmatrix} \mathrm{tr}(\mathbf{R}_1\hat{\mathbf{R}}_x) \\ \vdots \\ \mathrm{tr}(\mathbf{R}_K\hat{\mathbf{R}}_x) \\ \mathrm{tr}(\hat{\mathbf{R}}_x) \end{pmatrix}. \tag{24}$$

The main advantage of the test statistic (20) is that all the information on the sensed bandwidth is exploited for joint detection and estimation at a given band. Whereas filter-bank based detectors may suffer from adjacent channel leakage, the nuisance parameter formulation allows the detector to take advantage of the multi-frequency structure $\mathcal{M}$ for estimating both signal levels and noise variance. The frequency-domain asymptotic interpretation of the associated kernel $\mathcal{K}_{8,k}(\omega,\mathcal{M}) = \mathcal{K}_0\left[\hat{\gamma}_k\phi_k(\omega),\sum_{l\neq k}\hat{\gamma}_l\phi_l(\omega)+\hat{\sigma}_1^2\right]$ shows that the ML estimate of the noise variance flourishes together with the remaining bands as interference. We also note that for $K=1$, (23) and (24) reduce to (15) and (16), respectively.

6 Numerical Results

The sensing performance is assessed by means of experimental simulations modeling practical wideband cognitive radio scenarios. The GLRT spectrum sensing detectors derived in this work, which

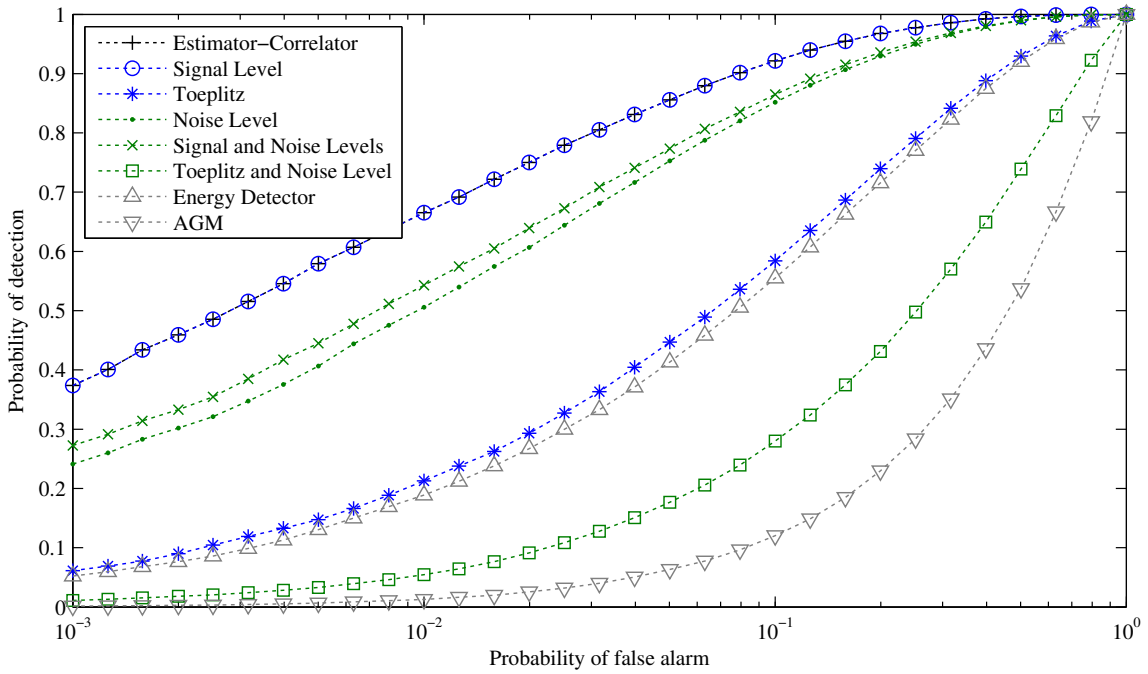

Figure 1: Receiver operating characteristics (ROC) of the wideband spectrum sensing detectors at $\rho_0 = -15$ dB.

are summarized in Table 6, are evaluated along with the energy detector [5], and the arithmetic-geometric mean (AGM) detector [17] based on the eigenvalues of the temporal correlation matrix.

In the sequel, the noise component is generated as i.d.d. zero-mean Gaussian vectors of length $N = 32$ and variance σ^2, whereas the signal component consists of $N = 32$ samples following the terrestrial digital video broadcasting (DVB-T) standard in the 2k-mode [37] of $K = 8$ channels, with a total power of γ. The sampling depth is set to $M = 2N = 64$, and 100,000 MonteCarlo trials are employed for averaging.

6.1 Sensing Performance

We first simulate the cognitive radio model (2) consisting of a secondary user equipped with a single sensing antenna. In this scenario, the relative occupation of the primary signal $S(t)$ is 25% of the sensing band, i.e., the spectral support of $\phi_s(\omega)$ is $\frac{1}{4}B$. Fig. 1 depicts the receiver operating characteristics (ROC) of the wideband GLRT spectrum sensing detectors derived in Sections 3 and 4, along with the energy detector and the AGM detector when the noise variance is perfectly calibrated by the secondary device, at a nominal $\rho_0 = -15$ dB.

It is noticed that the detectors with side-information on the second-order statistics of the pri-

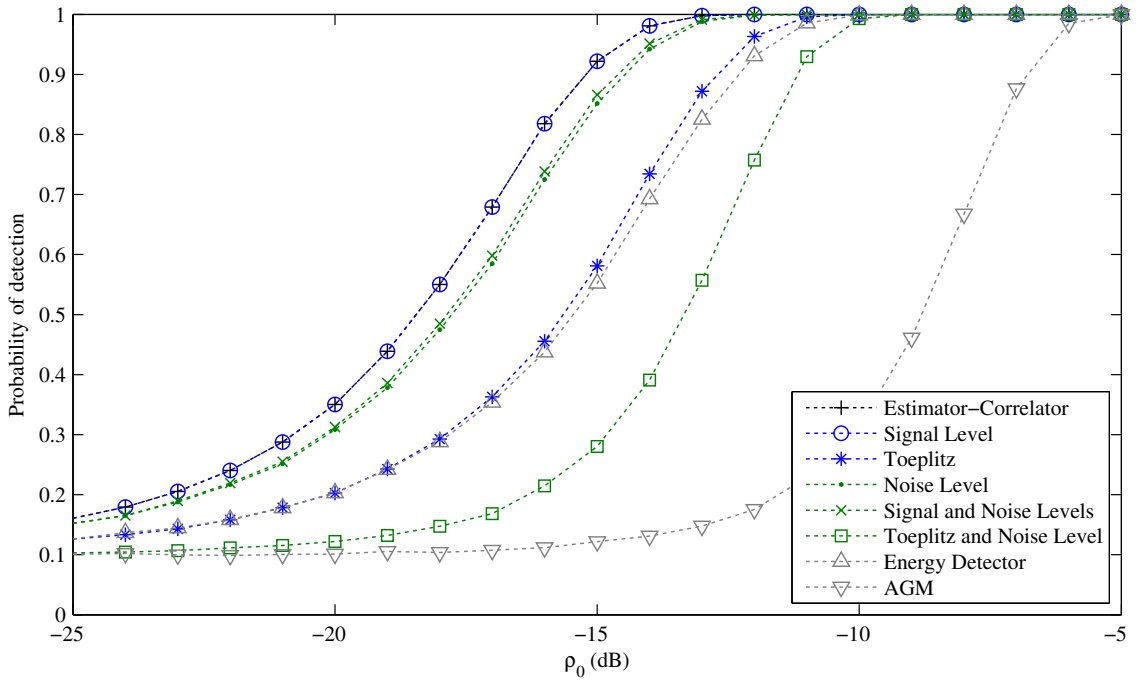

Figure 2: Probability of detection of the wideband spectrum sensing detectors versus average ρ_0 with false alarm level $\alpha = 0.1$.

mary systems signal, i.e., $\mathbf{R}_s$ or $\mathbf{R}_0$, provide sensing performance close the estimator-correlator upper-bound. It is observed that estimating the signal level incurs no performance loss. This is a known result, as the signal power, contrary to the noise power, is not a sufficient statistic [14]. As a result, the performance equivalence between the estimator-correlator and the signal level detector is common in the sequel. The accuracy in estimating the noise variance is reflected in maximum loss of 0.1 points in probability of detection along a wide range of probability of false alarm constraints.

It is interesting to observe that the signal and noise levels detector outperform the noise level detector. This behavior is due to the fact that the side-information on the signal power is an averaged statistics, therefore the true signal power of the observations may be inaccurate. Because the signal and noise levels detector performs ML estimation with two degrees of freedom, i.e., γ and σ^2, it shows a slight robustness in front of the noise level detector, which only exhibits ML estimation with one degree of freedom.

We further observe that the Toeplitz detector shows a slight gain with respect to the energy detector, because it exploits the correlation lags present in the off-diagonal of the sample correlation matrix, in addition to the energy computation of the main diagonal. Finally, as expected, the AGM detector's ROC curve is below that of the Toeplitz and noise variance detector, since the test

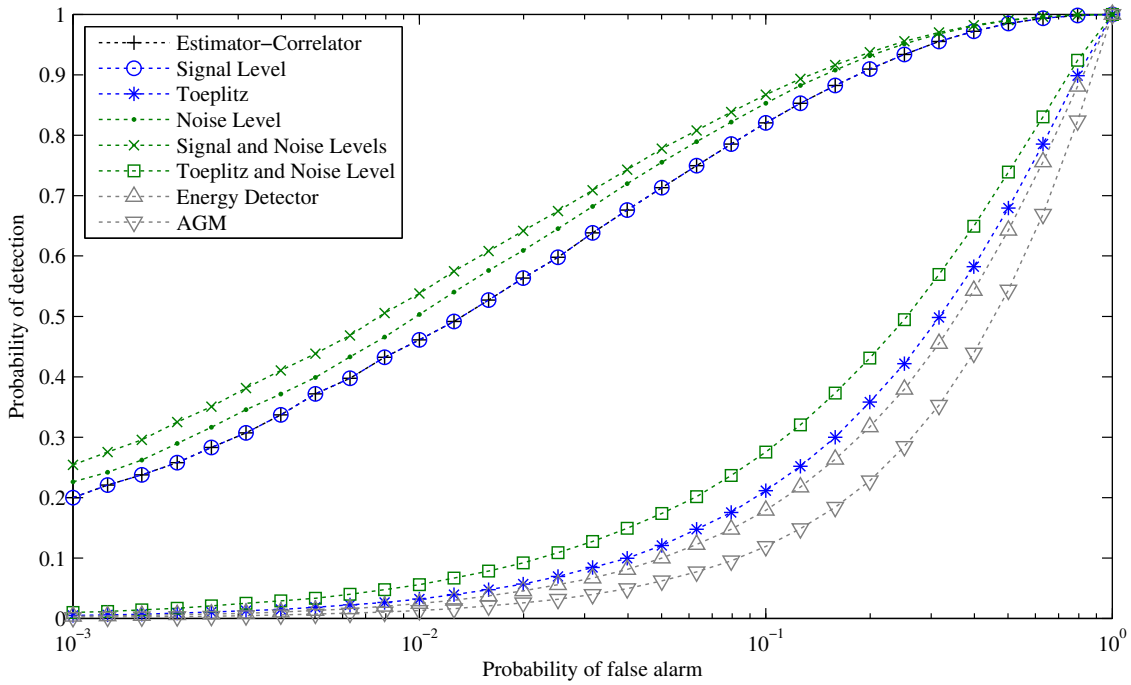

Figure 3: Receiver operating characteristics (ROC) of the wideband spectrum sensing detectors at $\rho_0 = -15$ dB with noise uncertainty $\kappa = 0.1$ dB.

statistic is less informative, e.g., does not exploit the Toeplitz structure of $\mathbf{R}_s$. Fig. 2 plots the probability of detection of the wideband GLRT spectrum sensing detectors versus average nominal ρ_0, at a fixed false alarm level of $\alpha = 0.1$. For a probability of detection requirement of 0.9, we see that the sensitivity of the detectors with known signal statistics is approximately 3 dB above the Toeplitz and energy detectors, and up to 10 dB with respect to the AGM detector.

6.2 Effect of Noise Uncertainty

In this work, the noise uncertainty level κ is modeled as the ratio between the a side-information noise variance σ^2_{ap} and the true noise variance σ^2, i.e., $\kappa \doteq \frac{\sigma^2_{ap}}{\sigma^2}$. In the sequel, we set $\kappa = 0.1$ dB. The ROC at $\rho_0 = -15$ dB, and the probability of detection with false alarm level $\alpha = 0.1$ of the GLRT spectrum sensing detectors are drawn in Fig. 3 and Fig. 4, respectively. A simple comparison between Fig. 1 and Fig. 3, and Fig. 2 and 4, respectively, outlines that the test statistics that assume perfect noise variance side-information suffer from performance degradation, whereas the rest of the detectors which incorporate noise variance ML estimation remain unaltered. This is a well-known result [36], and becomes the main motivation for the spectrum sensing detectors derived

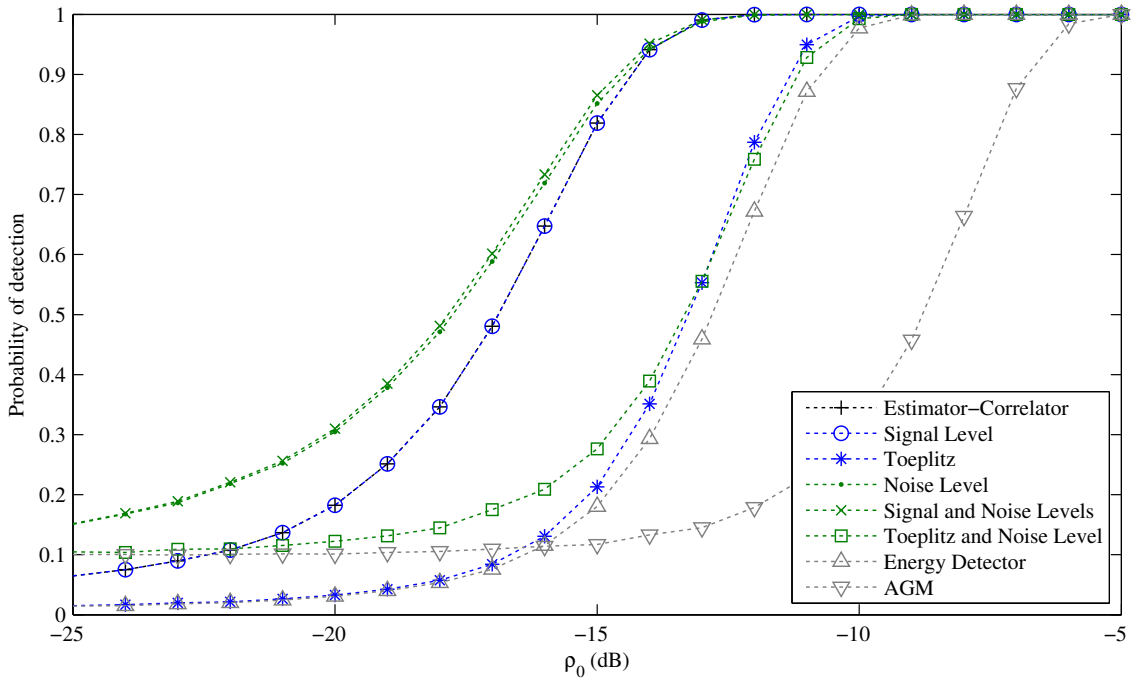

Figure 4: Probability of detection of the wideband spectrum sensing detectors versus average ρ_0 with false alarm level $\alpha = 0.1$ and noise uncertainty $\kappa = 0.1$ dB.

in Section 4. As appreciated in both figures, the performance curves of the estimator-correlator and the signal level detectors are displaced below the signal level and noise variance, and noise variance detectors. Likewise, the Toeplitz and energy detectors incur a penalty of approximately 2-3 dB of SNR sensibility, as seen by comparing Fig. 2 and Fig. 4.

6.3 Occupation

We now study the ROC interpretation of the wideband GLRT spectrum sensing detectors with fixed $\rho_0 = -15$ dB, in two opposite conditions of primary systems' relative occupation. As depicted in Fig. 5, the relative occupations of 12.5%, and 62.5% have been considered. By comparing both situations, it can be concluded that for a fixed noise and signal powers, spectrum sensing is a more challenging task when the primary users' signal is more spread over the sensed bandwidth. This effect is more remarkable for the detectors that exploit temporal correlation (e.g., the signal level, noise level, signal and noise levels, and toeplitz and noise level detectors) because temporal correlation decays with frequency occupation.

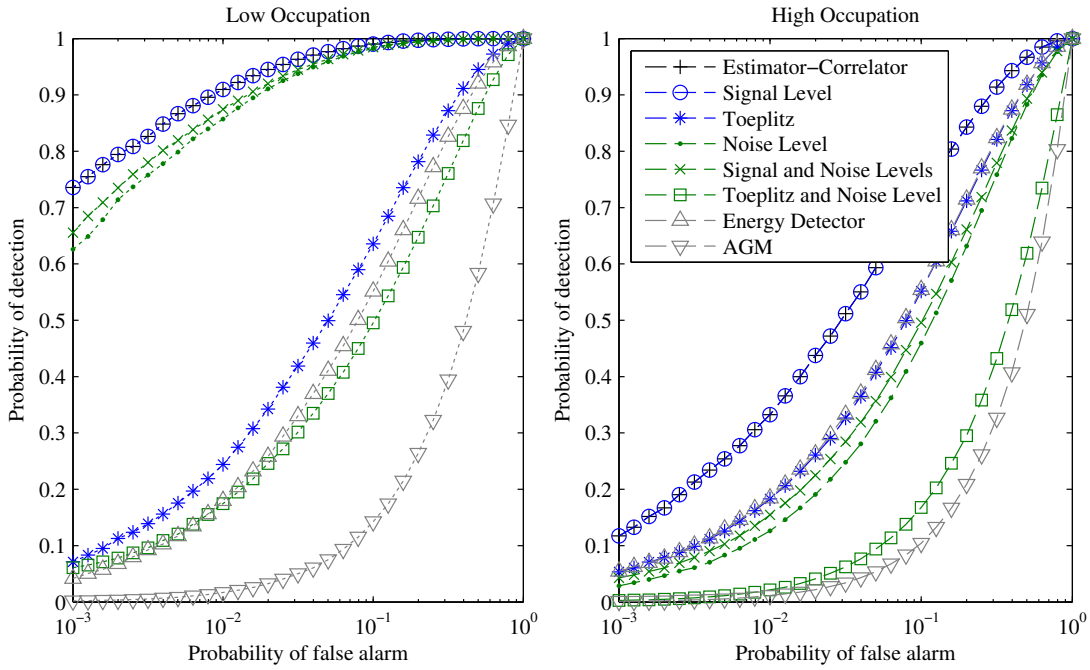

Figure 5: Receiver operating characteristics (ROC) of the wideband spectrum sensing detectors at $\rho_0 = -15$ dB with low (12.5%) and high (62.5%) primary systems relative occupation.

6.4 Multi-Frequency Systems

Finally, we evaluate the performance of the GLRT spectrum sensing detectors for multi-frequency systems. We consider a cognitive radio network with primary systems based on the terrestrial digital video broadcasting (DVB-T) standard in the 2k-mode in an example with $K = 8$ channels when sensing an arbitrary channel. For comparison reasons, we also add the nuisance estimator-correlator, i.e., the test statistic (21) with perfect side-information on $(\gamma_1, \ldots, \gamma_K)$. We define the SNR at the k-th channel as $\rho_{0,k} \doteq \frac{\gamma_k}{\sigma^2}$, with $\sum_{k=1}^{K} \rho_{0,k} = \rho_0$. On the one hand, the sensing performance of the multi-frequency GLRT spectrum sensing detectors derived in Section 5 is depicted in Fig. 6. It can be highlighted that, analogous to the wideband detectors, the side-information on the normalized correlation matrices $\mathbf{R}_k$ is the most informative statistic on the primary users' signal as the multi-frequency detector (21) incurs roughly no sensing loss in estimating the signal levels when the noise variance is perfectly known. However, the degradation of the multi-frequency detector due to noise variance estimation can be clearly appreciated in both figures. Whereas in terms of sensitivity the performance loss is roughly only 1-2 dB in SNR, the ROC for very restrictive false alarm levels incurs a large penalty. The main reason for this last appreciation is that the prob-

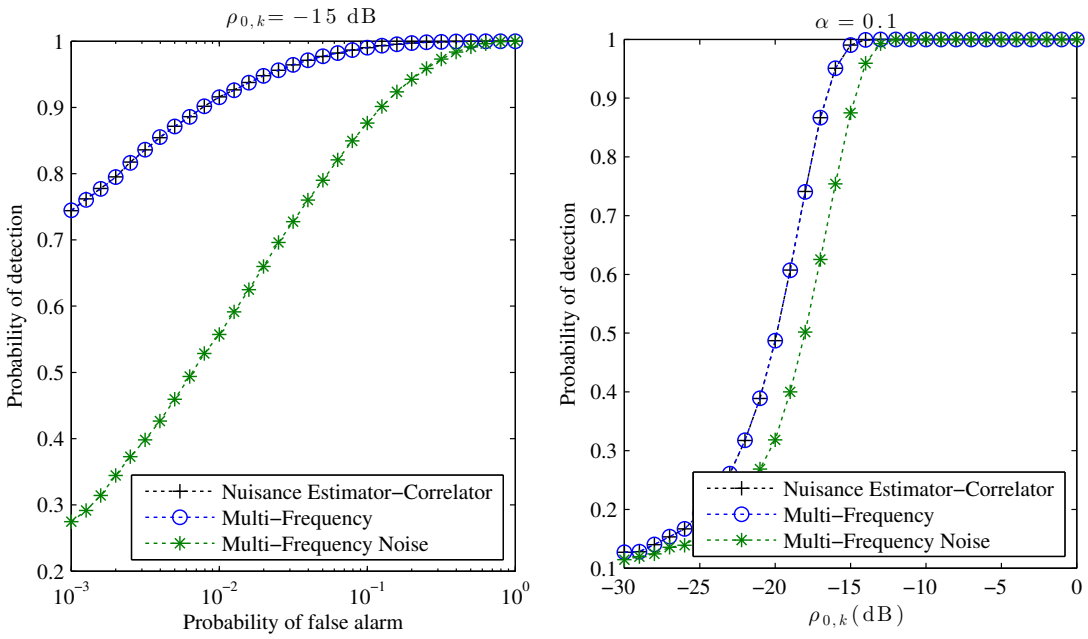

Figure 6: Sensing performance of multi-frequency systems.

ability of false alarm depends on the remaining frequency contributions, whose estimates become highly sensitive to the noise variance computation. We further show in Fig. 7 how the kernels actuate over the periodogram of the observations in the multi-frequency detector when sensing the 3rd band with $\gamma_1 = \gamma_3 = \gamma_7$, $\gamma_2 = \gamma_4 = \gamma_6 = \gamma_8 = 0$ and γ_5 with slightly more power As it can be appreciated, the kernel $\mathcal{K}_{7,k}(\omega, \mathcal{M})$ at $k = 3$ keeps the spectral shape of the estimator-correlator detector with a small shift and scaling. Both kernels show how they are affected by the spectral information outside the sensing frequency, because they are incorporated in $\phi_\nu(\omega)$ of $\mathcal{K}_{7,k}(\omega, \mathcal{M})$, along with the additive thermal noise. Hence, as an example, we can observe the effort of the kernels in diminishing the contribution of the signals around ω_5 and ω_7 while augmenting the focus on the detected channel, i.e., on ω_3.

7 Conclusions

In this paper, we have investigated the problem of spectrum sensing in wideband cognitive radios. Under the low-SNR assumption, we have derived a unified framework based on the frequency-domain asymptotic interpretation of the optimal GLRT spectrum sensing detectors. This unified framework uniquely consists of a kernel inherent to the detector, and the periodogram of the observations. We have further obtained the corresponding kernels for a variety of scenarios of practical

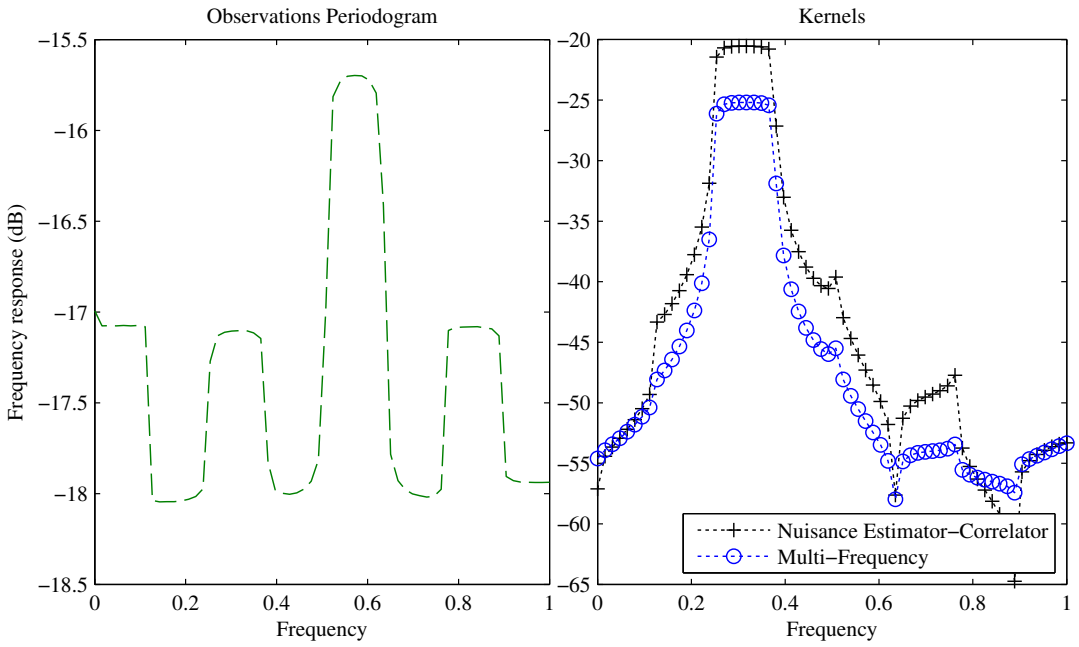

Figure 7: Frequency-domain interpretation of the kernels in multi-frequency spectrum sensing detectors at average $\rho_{0,k} = -15$ dB.

interest by obtaining closed-form ML estimates of the unknown parameters, including the signal level and noise variance, and multi-frequency systems. Theoretical interpretations and simulation results show that the primary signal's second order statistics constitute the most informative statistics for detection. Finally, we have seen that while noise variance estimation guarantees robustness in front of noise uncertainty, the detection kernel takes advantage of the spectral information contained over all the sensed bandwidth.

8 Acknowledgements

This work has been partially funded by the Spanish Government under TEC2010-21245-C02-01 (DYNACS), CONSOLIDER INGENIO CSD2008-00010 (COMONSENS), CENIT CEN-20101019 (THOFU), and the Catalan Government (DURSI) under Grant 2009SGR1236 and Fellowship FI-2010.

A Proof of Main Contribution

First, we proof that for asymptotically $\rho_0 \to 0$, the GLRT (3) is of the form $T(\mathbf{X}, \Theta) = \mathrm{tr}(\mathbf{K}\hat{\mathbf{R}}_x)$. Consider the GLRT (3) for the spectrum sensing problem (2) under the Gaussian assumption, i.e.,

$$L(\mathbf{X}) = \frac{p(\mathbf{X}|\hat{\mathbf{R}}_s, \hat{\sigma}_1^2, \mathcal{H}_1)}{p(\mathbf{X}|\hat{\sigma}_0^2, \mathcal{H}_0)} = \frac{\det(\hat{\sigma}_0^2\mathbf{I})^M}{\det(\hat{\mathbf{R}}_s + \hat{\sigma}_1^2\mathbf{I})^M} \times \frac{\exp \mathrm{tr}(-\mathbf{X}^H(\hat{\mathbf{R}}_s + \hat{\sigma}_1^2\mathbf{I})^{-1}\mathbf{X})}{\exp \mathrm{tr}(-\mathbf{X}^H(\hat{\sigma}_0^2\mathbf{I})^{-1}\mathbf{X})}.$$

Taking the logarithm and defining $\hat{\mathbf{R}}_x \doteq \frac{1}{M}\mathbf{X}\mathbf{X}^H$, after grouping terms we obtain

$$\frac{1}{M}\log L(\mathbf{X}) = \mathrm{tr}\left(\left(\frac{1}{\hat{\sigma}_0^2}\mathbf{I} - (\hat{\mathbf{R}}_s + \hat{\sigma}_1^2\mathbf{I})^{-1}\right)\hat{\mathbf{R}}_x\right) + \log\left(\frac{\hat{\sigma}_0^2}{\hat{\sigma}_1^2}\right) - \log\det\left(\mathbf{I} + \frac{1}{\hat{\sigma}_1^2}\mathbf{R}_s\right). \tag{25}$$

Approximating $\hat{\sigma}_0^2 \approx \hat{\sigma}_1^2$ and $\log\det\left(\mathbf{I} + \frac{1}{\hat{\sigma}_1^2}\hat{\mathbf{R}}_s\right) \approx \rho_0 \mathrm{tr}(\hat{\mathbf{R}}_s) \approx 0$, asymptotically as $\rho_0 \to 0$, and applying the inversion lemma $(\hat{\mathbf{R}}_s + \hat{\sigma}_1^2\mathbf{I})^{-1} = \frac{1}{\hat{\sigma}_1^2}\mathbf{I} - \frac{1}{\hat{\sigma}_1^4}\hat{\mathbf{R}}_s(\frac{1}{\hat{\sigma}_1^2}\hat{\mathbf{R}}_s + \mathbf{I})^{-1} = \frac{1}{\hat{\sigma}_1^2}\mathbf{I} - \frac{1}{\hat{\sigma}_1^2}\hat{\mathbf{R}}_s(\hat{\mathbf{R}}_s + \hat{\sigma}_1^2\mathbf{I})^{-1}$, we obtain

$$\frac{1}{M}\log L(\mathbf{X}) \approx \mathrm{tr}\left(\frac{1}{\hat{\sigma}_1^2}\hat{\mathbf{R}}_s(\hat{\sigma}_1^2\mathbf{I} + \hat{\mathbf{R}}_s)^{-1}\hat{\mathbf{R}}_x\right) \doteq \mathrm{tr}\left(\mathbf{K}\hat{\mathbf{R}}_x\right). \tag{26}$$

For the second part of the proof, we recall that for large data records (i.e., as $N \to \infty$) in (2), it is established in [14, Ch. 5, Sec. 5] though approximating the probability density function (PDF) of $\mathbf{X}$ that log-likelihood decision statistic (26) can be approximated as (5), where $\mathcal{K}(\omega, \Theta)$ is the asymptotic continuous-frequency transform of the second-order statistic $\mathbf{K}$ given by (6), and $P(\omega)$ is the continuous-frequency periodogram of $\mathbf{X}$.

B Derivation of ML Estimates

This Appendix reports a sketch on the derivation of the ML estimates employed in this paper. An important result required in the following derivations is the low-SNR approximation

$$\left(\mathbf{R}_s + \sigma^2\mathbf{I}\right)^{-1} \approx \frac{1}{\sigma^2}\left(\mathbf{I} - \frac{1}{\sigma^2}\mathbf{R}_s\right). \tag{27}$$

B.1 Derivation of (9)

The ML estimate of γ under $\mathcal{H}_1$ for the spectrum sensing problem (2) is given by

$$\hat{\gamma} = \arg\min_{\gamma} \ \log\det(\gamma\mathbf{R}_0 + \sigma^2\mathbf{I}) + \mathrm{tr}\left((\gamma\mathbf{R}_0 + \sigma^2\mathbf{I})^{-1}\hat{\mathbf{R}}_x\right)$$

subject to $\gamma \geq 0$. By taking the derivative with respect to γ and set it to zero we obtain and equation whose solution is equivalent to (22), proved in [33, Appendix B] for $K = 1$, i.e., $\mathrm{tr}(\mathbf{R}^2)\gamma = \mathrm{tr}(\mathbf{R}_1\hat{\mathbf{R}}_x) - \sigma^2 N$, which results in (9).

B.2 Derivation of (12)

Let $\mathbf{R}_s[\boldsymbol{\beta}]$ be the decomposition of $\mathbf{R}_s$ given by (10). The ML estimate of the coefficients if given by

$$\hat{\boldsymbol{\beta}} = \arg\min_{\boldsymbol{\beta}} \log\det\left(\mathbf{R}_s[\boldsymbol{\beta}] + \sigma^2\mathbf{I}\right) + \mathrm{tr}\left(\left(\mathbf{R}_s[\boldsymbol{\beta}] + \sigma^2\mathbf{I}\right)^{-1}\hat{\mathbf{R}}_x\right),$$

with the additional constraint $\beta_0 \in \mathbb{R}_+$. By making use of the derivative properties, we take the derivative of the objective with respect to $\beta^*_{n'}$, which leads to the equation

$$\mathrm{tr}\left(\left(\mathbf{R}_s[\boldsymbol{\beta}] + \sigma^2\mathbf{I}\right)^{-1}\mathbf{T}_{n'}\right) - \mathrm{tr}\left(\left(\mathbf{R}_s[\boldsymbol{\beta}] + \sigma^2\mathbf{I}\right)^{-1}\mathbf{T}_{n'}\left(\mathbf{R}_s[\boldsymbol{\beta}] + \sigma^2\mathbf{I}\right)^{-1}\hat{\mathbf{R}}_x\right) = 0,$$

for $0 \leq n \leq N-1$. In the wideband regime, we further make use of Approximation (27) to approximate the following terms

$$\mathrm{tr}\left(\left(\mathbf{R}_s[\boldsymbol{\beta}] + \sigma^2\mathbf{I}\right)^{-1}\mathbf{T}_{n'}\right) \approx \frac{1}{\sigma^2}\mathrm{tr}(\mathbf{T}_{n'}) - \frac{1}{\sigma^4}\mathrm{tr}\left(\mathbf{R}_s[\boldsymbol{\beta}]\mathbf{T}_{n'}\right),$$

and

$$\mathrm{tr}\left(\left(\mathbf{R}_s[\boldsymbol{\beta}] + \sigma^2\mathbf{I}\right)^{-1}\mathbf{T}_{n'}\left(\mathbf{R}_s[\boldsymbol{\beta}] + \sigma^2\mathbf{I}\right)^{-1}\hat{\mathbf{R}}_x\right) \approx \frac{1}{\sigma^4}\mathrm{tr}(\mathbf{T}_{n'}\hat{\mathbf{R}}_x) - \frac{2}{\sigma^6}\mathrm{tr}\left(\mathbf{R}_s[\boldsymbol{\beta}]\mathbf{T}_{n'}\hat{\mathbf{R}}_x\right).$$

Applying the former approximations, we obtain that the ML estimate of $\mathbf{R}_s$ accomplishes

$$\frac{2}{\sigma^6}\mathrm{tr}\left(\mathbf{R}_s[\boldsymbol{\beta}]\mathbf{T}_{n'}\hat{\mathbf{R}}_x\right) - \frac{1}{\sigma^4}\mathrm{tr}\left(\mathbf{R}_s[\boldsymbol{\beta}]\mathbf{T}_{n'}\right) = \frac{1}{\sigma^4}\mathrm{tr}(\mathbf{T}_{n'}\hat{\mathbf{R}}_x) - \frac{1}{\sigma^2}\mathrm{tr}(\mathbf{T}_{n'}).$$

We further make use of the low-SNR approximation with the left-hand side of the former equation. Noting that $\mathrm{tr}(2\hat{\mathbf{R}}_x - \sigma^2\mathbf{I}) \approx \sigma^2\mathbf{I}$, it reduces, after multiplying both sides by σ^2, to $\mathrm{tr}(\mathbf{R}_s[\boldsymbol{\beta}]\mathbf{T}_{n'}) = \mathrm{tr}(\mathbf{T}_{n'}\hat{\mathbf{R}}_x) - \sigma^2\mathrm{tr}(\mathbf{T}_{n'})$. Now, we make use of the orthogonality of $\mathcal{T}$, to note that the term $\mathrm{tr}(\mathbf{R}_s[\boldsymbol{\beta}]\mathbf{T}_{n'})$, using the decomposition (10), equals to $\beta_n\mathrm{tr}(\mathbf{T}_n^T\mathbf{T}_n)$, i.e., only the term $n = n'$ survives. Finally, we get the equations $\beta_n\mathrm{tr}(\mathbf{T}_n^T\mathbf{T}_n) = \mathrm{tr}(\mathbf{T}_n\hat{\mathbf{R}}_x) - \sigma^2\mathrm{tr}(\mathbf{T}_n)$, which for $n = 0$ as $\mathbf{T}_0 = \mathbf{I}$ gives β_0 in (12a), and for $n \geq 1$ as $\mathrm{tr}(\mathbf{T}_n) = 0$ gives β_n in (12b).

B.3 Derivation of (16)

The ML estimates of γ and σ^2 are given by the convex optimization problem

$$\hat{\gamma}, \hat{\sigma}_1^2 = \arg\min_{\gamma,\sigma^2} \ \log\det(\gamma\mathbf{R}_0 + \sigma^2\mathbf{I}) + \mathrm{tr}\left((\gamma\mathbf{R}_0 + \sigma^2\mathbf{I})^{-1}\hat{\mathbf{R}}_x\right).$$

The solution is equivalent to (24) for $K = 1$, proved in [33, Appendix C], i.e., the system of equations formed by $\gamma\mathrm{tr}(\mathbf{R}_0^2) + \sigma^2 N = \mathrm{tr}(\mathbf{R}_0\hat{\mathbf{R}}_x)$, and $\gamma N + \sigma^2 N = \mathrm{tr}(\hat{\mathbf{R}}_x)$. After some mathematical manipulations, we obtain that the solutions are given by (16).

B.4 Derivation of (18)

The ML estimate of the coefficients and the noise variance are given by the optimization problem

$$\hat{\boldsymbol{\beta}}, \hat{\sigma}_1^2 = \arg\min_{\boldsymbol{\beta},\sigma^2} \log\det\left(\mathbf{R}_s[\boldsymbol{\beta}] + \sigma^2\mathbf{I}\right) + \mathrm{tr}\left(\left(\mathbf{R}_s[\boldsymbol{\beta}] + \sigma^2\mathbf{I}\right)^{-1}\hat{\mathbf{R}}_x\right),$$

with the additional constraint $\beta_0 \in \mathbb{R}_+$. As the problem is convex on $\boldsymbol{\beta}$ and σ^2, we take the derivative of the objective with respect to β_n^* and σ^2. On the one hand, the derivative with respect to β_n^* has been derived in Appendix B.2 and, after some mathematical manipulations and making use of Approximation (27) and the orthogonality of $\mathcal{T}$, reduces to $\beta_n \mathrm{tr}(\mathbf{T}_n^T\mathbf{T}_n) + \sigma^2\mathrm{tr}(\mathbf{T}_n) = \mathrm{tr}(\mathbf{T}_n\hat{\mathbf{R}}_x)$, for $0 \leq n \leq N-1$. Hence, for $n \geq 1$, we proof (18b) because $\mathrm{tr}(\mathbf{T}_n) = 0$. For $n = 0$, we have $\beta_0 + \sigma^2 = \frac{1}{N}\mathrm{tr}(\hat{\mathbf{R}}_x)$, together with the derivative with respect to σ^2, i.e., $\mathrm{tr}\left(\left(\mathbf{R}_s[\boldsymbol{\beta}] + \sigma^2\mathbf{I}\right)^{-1}\right) - \mathrm{tr}\left(\left(\mathbf{R}_s[\boldsymbol{\beta}] + \sigma^2\mathbf{I}\right)^{-2}\hat{\mathbf{R}}_x\right) = 0$. After applying Approximation (27), we obtain the following approximations $\mathrm{tr}\left(\left(\mathbf{R}_s[\boldsymbol{\beta}] + \sigma^2\mathbf{I}\right)^{-1}\right) \approx \frac{1}{\sigma^2}N - \frac{1}{\sigma^4}\mathrm{tr}\left(\mathbf{R}_s[\boldsymbol{\beta}]\right)$, and

$$\mathrm{tr}\left(\left(\mathbf{R}_s[\boldsymbol{\beta}] + \sigma^2\mathbf{I}\right)^{-1}\mathbf{T}_{n'}\left(\mathbf{R}_s[\boldsymbol{\beta}] + \sigma^2\mathbf{I}\right)^{-1}\hat{\mathbf{R}}_x\right) \approx \frac{1}{\sigma^4}\mathrm{tr}(\hat{\mathbf{R}}_x) - \frac{2}{\sigma^6}\mathrm{tr}\left(\mathbf{R}_s[\boldsymbol{\beta}]\hat{\mathbf{R}}_x\right).$$

Finally, noting that at the low-SNR regime we can further approximate $\mathrm{tr}(2\hat{\mathbf{R}}_x - \sigma^2\mathbf{I}) \approx \sigma^2\mathbf{I}$, we obtain $\mathrm{tr}(\mathbf{R}_s[\boldsymbol{\beta}]) + \sigma^2 N = \mathrm{tr}(\hat{\mathbf{R}}_x)$. As $\mathrm{tr}(\mathbf{R}_s[\boldsymbol{\beta}]) = \beta_0 N$, we obtain, again, $\beta_0 + \sigma^2 = \frac{1}{N}\mathrm{tr}(\hat{\mathbf{R}}_x)$. Hence, employing the matrix decomposition $\mathcal{T}$, we note that both β_0 and σ^2 account for the white component of the received observations, and the ML estimates cannot be found further than $\hat{\beta}_0 + \hat{\sigma}_1^2 = \frac{1}{N}\mathrm{tr}(\hat{\mathbf{R}}_x)$, proving (18b).

References

[1] FCC. Notice of proposed rule making and order. ET Docket No. 03-222, Federal Communications Commission, December 2003.

[2] III Mitola, J. and G. Q. Maguire. Cognitive radio: making software radios more personal. *IEEE Personal Commun. Mag.*, 6(4):13–18, August 1999.

[3] A. Goldsmith, S. A. Jafar, I. Maric, and S. Srinivasa. Breaking spectrum gridlock with cognitive radios: An information theoretic perspective. *Proc. of the IEEE*, 97(5):894–914, May 2009.

[4] E. Axell, G. Leus, E.G. Larsson, and H.V. Poor. Spectrum sensing for cognitive radio : State-of-the-art and recent advances. *IEEE Signal Process. Mag.*, 29(3):101–116, May 2012.

[5] H. V. Poor. *An introduction to signal detection and estimation*. Springer-Verlag, New York, NY, 1994.

[6] P.D. Sutton, K.E. Nolan, and L.E. Doyle. Cyclostationary signatures in practical cognitive radio applications. *IEEE J. Sel. Areas Commun.*, 26(1):13–24, January 2008.

[7] J. G. Proakis. *Digital Communications*. Science/Engineering/Math. McGraw-Hill, 4th edition, August 2000.

[8] S. Kay. A new proof of the Neyman-Pearson theorem using the EEF and the vindication of Sir R. Fisher. *IEEE Signal Process. Lett.*, 19(8):451–454, August 2012.

[9] G.V. Moustakides, G.H. Jajamovich, A. Tajer, and Xiaodong Wang. Joint detection and estimation: Optimum tests and applications. *IEEE Trans. Inf. Theory*, 58(7):4215–4229, July 2012.

[10] J. Font-Segura and X. Wang. GLRT-based spectrum sensing for cognitive radio with prior information. *IEEE Trans. Commun.*, 58(7):2137–2146, July 2010.

[11] H. Sun, A. Nallanathan, C.-X. Wang, and Y. Chen. Wideband spectrum sensing for cognitive radio networks: a survey. *IEEE Trans. Wireless Commun.*, 20(2):74–81, April 2013.

[12] S. Verdu. Spectral efficiency in the wideband regime. *IEEE Trans. Inf. Theory*, 48(6):1319–1343, June 2002.

[13] B. Porat. *Digital Processing of Random Signals. Theory and Methods*. Dover Publications, February 2008.

[14] S. M. Kay. *Fundamentals of statistical signal processing*, volume 2 (detection theory). Prentice Hall, Upper Saddle River, NJ, 1998.

[15] W. A. Gardner, A. Napolitano, and L. Paura. Cyclostationarity: Half a century of research. *IEEE Signal Process. Mag.*, 86(4):639–697, April 2006.

[16] Z. Quan, W. Zhang, S. J. Shellhammer, and A. H. Sayed. Optimal spectral feature detection for spectrum sensing at very low-SNR. *IEEE Trans. Commun.*, 59(1):201–212, January 2011.

[17] R. Zhang, T. J. Lim, Y-C. Liang, and Y. Zeng. Multi-antenna based spectrum sensing for cognitve radios: a GLRT approach. *IEEE Trans. Commun.*, 58(1):84–88, January 2010.

[18] P. Wang, J. Fang, N. Han, and H. Li. Multiantenna-assisted spectrum sensing for cognitive radio. *IEEE Trans. Veh. Technol.*, 59(4):1791–1800, May 2010.

[19] A. Taherpour, M. Nasiri-Kenari, and S. Gazor. Multiple antenna spectrum sensing in cognitive radios. *IEEE Trans. Wireless Commun.*, 9(2):814–823, February 2010.

[20] D. Ramírez, J. Vía, and I. Santamaria. Multiantenna spectrum sensing: The case of wideband rank-one primary signals. In *IEEE Sensor Array and Multichannel Signal Process. Workshop (SAM)*, October 2010.

[21] G. Vázquez-Vilar, R. López-Valcarce, and J. Sala. Multiantenna spectrum sensing exploiting spectral a priori information. *IEEE Trans. Wireless Commun.*, 10(12):4345–4355, December 2011.

[22] D. Ramírez, G. Vázquez-Vilar, R. López-Valcarce, J. Vía, and I. Santamaría. Detection of rank-P signals in cognitive radio networks with uncalibrated multiple antennas. *IEEE Trans. Signal Process.*, 59(8):3764–3774, August 2011.

[23] L. Shen, H. Wang, W. Zhang, and Z. Zhao. Multiple antennas assisted blind spectrum sensing in cognitive radio channels. *IEEE Commun. Lett.*, 16(1):92–94, January 2012.

[24] J. Sala-Alvarez, G. Vázquez-Vilar, and R. López-Valcarce. Multiantenna GLR detection of rank-one signals with known power spectrum in white noise with unknown spatial correlation. *IEEE Trans. Signal Process.*, 60(6):3065–3078, June 2012.

[25] S. Sedighi, A. Taherpour, and S.S.M. Monfared. Bayesian generalised likelihood ratio test-based multiple antenna spectrum sensing for cognitive radios. *IET Commun.*, 7(18):2151–2165, 2013.

[26] D. Ramírez, J. Vía, I. Santamaría, and L.L. Scharf. Locally most powerful invariant tests for correlation and sphericity of Gaussian vectors. *IEEE Trans. Inf. Theory*, 59(4):2128–2141, April 2013.

[27] P. Zhang and R. Qiu. GLRT-based spectrum sensing with blindly learned feature under rank-1 assumption. *IEEE Trans. Commun.*, 61(1):87–96, January 2013.

[28] S. Zheng, P.-Y. Kam, Y.-C. Liang, and Y. Zeng. Spectrum sensing for digital primary signals in cognitive radio: A Bayesian approach for maximizing spectrum utilization. *IEEE Trans. Wireless Commun.*, 12(4):1774–1782, April 2013.

[29] M. Naraghi-Pour and T. Ikuma. Autocorrelation-based spectrum sensing for cognitive radios. *IEEE Trans. Veh. Technol.*, 59(2):718–733, February 2010.

[30] X. Yang, K. Lei, S. Peng, and X. Cao. Blind detection for primary user based on the sample covariance matrix in cognitive radio. *IEEE Commun. Lett.*, 15(1):40–42, January 2011.

[31] S. W. Boyd, J. M. Frye, M. B. Pursley, and T. C. Royster IV. Spectrum monitoring during reception in dynamic spectrum access cognitive radio networks. *IEEE Trans. Commun.*, 60(2):547–558, February 2012.

[32] W. Zhang, H.V. Poor, and Z. Quan. Frequency-domain correlation: An asymptotically optimum approximation of quadratic likelihood ratio detectors. *IEEE Trans. Signal Process.*, 58(3):969–979, March 2010.

[33] J. Font-Segura, G. Vázquez, and J. Riba. Multi-frequency GLRT spectrum sensing for wideband cognitive radio. In *IEEE Int. Conf. Commun. (ICC)*, June 2011.

[34] J. Font-Segura, J. Riba, J. Villares, and G. Vázquez. Quadratic sphericity test for blind detection over time-varying frequency-selective channels. In *IEEE International Conference on Acoustics, Speech and Signal Processing (ICASSP)*, May 2013.

[35] J. Villares and G. Vázquez. The Gaussian assumption in second-order estimation problems in digital communications. *IEEE Trans. Signal Process.*, 55(10):4994–5002, October 2007.

[36] R. Tandra and A. Sahai. SNR walls for signal detection. *IEEE J. Sel. Topics Signal Process.*, 2(1):4–17, February 2008.

[37] ETSI. Digital Video Broadcasting (DVB); framing structure, channel coding and modulation for digital terrestrial television (DVB-T). Technical Report EN 300 744 V1.5.1, European Telecommunications Standards Institute (ETSI), June 2004. http://www.etsi.org/deliver/etsi_en/300700_300799/300744/01.05.01_40/en_300744v010501o.pdf.